Bioactive Materials 25 (2023) 460–471

Contents lists available at ScienceDirect

Bioactive Materials

journal homepage: www.keaipublishing.com/en/journals/bioactive-materials

Multifunctional hydrogel enhances bone regeneration through sustained release of Stromal Cell-Derived Factor-1α and exosomes

Lang Chen [a,b,c,1], Chenyan Yu [a,b,1], Yuan Xiong [a,b,1], Kai Chen [a,d,1], Pei Liu [a,d], Adriana C. Panayi [e], Xiufeng Xiao [a,d,****], Qian Feng [a,d,f,***], Bobin Mi [a,b,**], Guohui Liu [a,b,*]

[a] Department of Orthopaedics, Union Hospital, Tongji Medical College, Huazhong University of Science and Technology, Wuhan, 430022, China
[b] Hubei Province Key Laboratory of Oral and Maxillofacial Development and Regeneration, Wuhan, 430022, China
[c] Department of Physics and Center for Hybrid Nanostructure (CHyN), University of Hamburg, Luruper Chaussee 149, Hamburg 22761, Hamburg, Germany
[d] Fujian Provincial Key Laboratory of Advanced Materials Oriented Chemical Engineering, College of Chemistry and Materials Science, Fujian Normal University, Fuzhou, Fujian, 350007, China
[e] Division of Plastic Surgery, Brigham and Women's Hospital, Harvard Medical School, Boston, MA, 02215, USA
[f] Key Laboratory of Biorheological Science and Technology, Ministry of Education College of Bioengineering, Chongqing University, Chongqing, 400044, China

ARTICLE INFO

Keywords:
Hydrogel
SDF-1α
Macrophage
Exosomes
Fracture healing

ABSTRACT

Fracture nonunion remains a great challenge for orthopedic surgeons. Fracture repair comprises of three phases, the inflammatory, repair and remodeling stage. Extensive advancements have been made in the field of bone repair, including development of strategies to balance the M1/M2 macrophage populations, and to improve osteogenesis and angiogenesis. However, such developments focused on only one or the latter two phases, while ignoring the inflammatory phase during which cell recruitment occurs. In this study, we combined Stromal Cell-Derived Factor-1α (SDF-1α) and M2 macrophage derived exosomes (M2D-Exos) with a hyaluronic acid (HA)-based hydrogel precursor solution to synthesize an injectable, self-healing, adhesive HA@SDF-1α/M2D-Exos hydrogel. The HA hydrogel demonstrated good biocompatibility and hemostatic ability, with the 4% HA hydrogels displaying great antibacterial activity against gram-negative *E. coli* and gram-positive *S. aureus* and Methicillin-resistant *Staphylococcus aureus* (MRSA). Synchronously and sustainably released SDF-1α and M2D-Exos from the HA@SDF-1α/M2D-Exos hydrogel enhanced proliferation and migration of human bone marrow mesenchymal stem cell (HMSCs) and Human Umbilical Vein Endothelial Cells (HUVECs), promoting osteogenesis and angiogenesis both in vivo and in vitro. Overall, the developed HA@ SDF-1α/M2D-Exos hydrogel was compatible with the natural healing process of fractures and provides a new modality for accelerating bone repair by coupling osteogenesis, angiogenesis, and resisting infection at all stages.

1. Introduction

Bone fractures are one of the most frequently encountered injuries of the musculoskeletal system, affecting over 18.3 million patients per year and costing close to $12,000 per complication in the US [1,2]. Although recent years have seen extensive advancements in therapy development, the rate of non-union is still reported to be around 5–10% of total fractures [3]. Bone regeneration strategies including recruiting M2

Peer review under responsibility of KeAi Communications Co., Ltd.

* Corresponding author. Department of Orthopaedics, Union Hospital, Tongji Medical College, Huazhong University of Science and Technology, Wuhan, 430022, China.
** Corresponding author. Department of Orthopaedics, Union Hospital, Tongji Medical College, Huazhong University of Science and Technology, Wuhan, 430022, China.
*** Corresponding author. Department of Orthopaedics, Union Hospital, Tongji Medical College, Huazhong University of Science and Technology, Wuhan, 430022, China.
**** Corresponding author. Department of Orthopaedics, Union Hospital, Tongji Medical College, Huazhong University of Science and Technology, Wuhan, 430022, China.
E-mail addresses: xfxiao@fjnu.edu.cn (X. Xiao), qianfeng@cqu.edu.cn (Q. Feng), mibobin@hust.edu.cn (B. Mi), liuguohui@hust.edu.cn (G. Liu).
[1] Co-first author: Lang Chen, Chenyan Yu, Yuan Xiong and Kai Chen contributed equally to this work.

https://doi.org/10.1016/j.bioactmat.2022.07.030
Received 24 May 2022; Received in revised form 24 July 2022; Accepted 27 July 2022
Available online 12 August 2022

macrophages, enhancing bone marrow mesenchymal stem cells (BMSCs) and HUVEC adhesion, spreading and proliferation, have been proposed and allowed clinical progress [4,5]. However, recent strategies mainly focus on the endochondral stage and coupled remodeling stage of fracture healing and accelerate fracture healing by strengthening the function of MSCs or HUVECs, while the inflammatory stage including M1/M2 transfer and cell recruitment have been poorly studied [6,7]. Given the importance and various roles of the different stages, the core of promoting fracture healing should be to coordinate and overall shorten the fracture repair process.

MSCs and endothelial cells are the two main cells in fracture healing involved in osteogenic differentiation and providing nutrition, respectively [4,8]. It has been reported that M1 macrophages play a major role in the recruitment of MSCs and vascular progenitor cells to the fracture site during the initial inflammatory reaction [9,10], which could be promoted by secreted chemokines including CCL2, CXCL8 and SDF-1 [11,12]. As one of the strongest chemokines, SDF-1 has been shown to recruit circulating bone marrow-derived osteoblast progenitor cells via the SDF-1/Chemokine receptor type 4 (CXCR4) pathway [13]. Lu et al. also found that bone targeted delivery of SDF-1 using nanoparticles can trigger MSC migration and accelerate osseous tissue accumulation in vivo [14].

Recently, exosomes have been widely used to alter cell function, including their ability to migrate and differentiate [15,16]. Our team have reported that M2 macrophage-derived exosomes (M2D-Exos) accelerate osteogenic differentiation both in vivo and in vitro, but it is still elusive whether M2D-Exos play a positive role in angiogenesis and there is no evidence that M2D-Exos is related to cell migration [17]. A challenge identified in our prior work is how to better preserve the activity of chemokines and Exos and release them slowly into the fracture site.

Recently, bioactive hydrogels have become a research hotspot in fracture healing [18], as they can act as carriers for bioactive small molecules to promote osteogenesis and angiogenesis, thereby playing a vital role in the repair and remodeling stage [19,20].

In the present study, we designed and produced an injectable, adhesive HA@SDF-1α/M2D-Exos hydrogel to act as a molecule carrier and showed it to induce a local antibacterial microenvironment conducive of fracture healing. Since different concentrations of hydrogels may have different characterizations, antibacterial activity and biocompatibility, 2%, 4% and 6% HA hydrogel was synthesized and studied respectively. Controlled-release of SDF-1α accelerated HMSC and HUVEC migration while M2D-Exos improved cell proliferation, HMSC mineral deposition and HUVEC tube formation. Collectively, the whole design was compatible with the natural healing process of fractures, accelerating fracture healing while limiting infection (Scheme 1).

2. Materials and methods

2.1. Hyaluronic acid (HA) modification

For the preparation of adipic acid dihydrazide-modified HA (HA-ADH), N-(3-Dimethy laminopropyl)-N′-ethylcarbodiimide hydrochloride (EDC, Macklin, China) and 1-hydroxy-benzotriazole (HOBT, J&K Scientific, China) were added into the solution of 1 wt% HA (MW = 70 kDa, Shandong Focusfreda Biotech Co., Ltd, China) in 4-Morpholineethanesulfonic acid (MES, Macklin, China) buffer (pH = 6.5) to activate the carboxyl groups in the backbone of HA. After 1 h of reaction, Adipic acid dihydrazide (ADH, Macklin, China) was also added into the mixture before 24 h of reaction. Then, the final product HA-ADH were obtained after three days of dialysis against deionized water (DI water) and three days of lyophilization.

As for the preparation of oxidized HA -quaternary ammonium (OHA-QA), OHA should be synthesized first. 0.6 g sodium periodate (NaIO4, AR, Macklin, China) was added to 100 mL HA solution (1 wt%) and stirred for 24 h in the dark at room temperature before three days of dialysis against Di water and three days of lyophilization. Then, the obtained OHA was reacted with Girard's reagent T (Aladdin, China) under pH = 4.5. The reaction solution also underwent three days of dialysis against Di water and three days of lyophilization before obtaining the dry product OHA-QA.

2.2. HA-based hydrogel fabrication

The hydrogel was conveniently fabricated by mixing the phosphate-buffered saline (PBS) solution of HA-ADH and OHA-QA at equal volumes by using a hand-made dual syringe. The different groups of the HA-based hydrogels were distinguished by their final solid content. For example, 2% HA based hydrogel was prepared by mixing 2 wt% HA-ADH and 2 wt % OHA-QA.

2.3. Hydrogel swelling ratio measurement

Different groups of HA-based hydrogels were immersed in 1 mL PBS separately. At specific points in time, we took out the hydrogel samples and removed the excess water from the surface with filter paper before recording the accurate weight of the samples. The wet and dried weight of these samples was marked as W_w and W_d, respectively. The swelling ratio was then calculated with the following equation: $(W_w\text{-}W_d)/W_d \times 100\%$

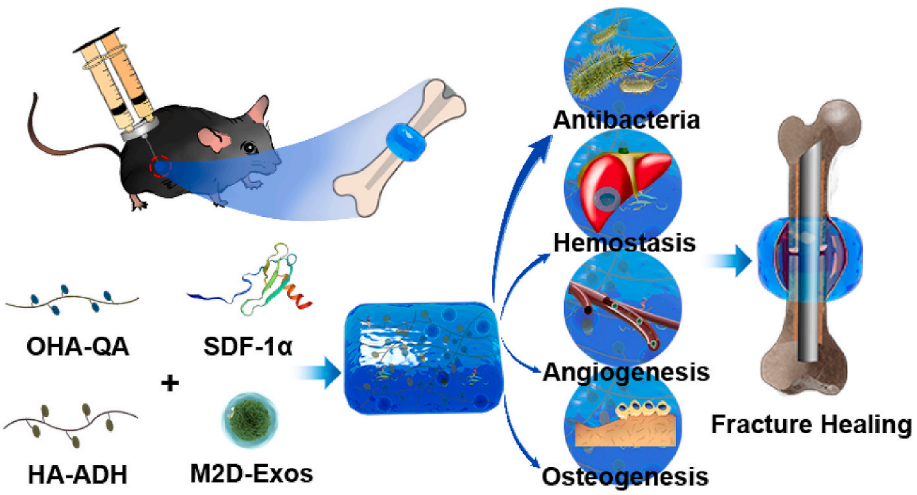

Scheme 1. The mechanisms underlying HA@SDF-1α/M2D-Exos hydrogel's ability to accelerate fracture healing. The HA@SDF-1α/M2D-Exos hydrogel can be constructed in situ through a mixed injection process. The hydrogel formed rapidly due to the hydrazone bond formation between the HA-ADH and the OHA-QA crosslinking, while the positively charged quaternary ammonium groups of the hydrogel provided a long-term antibacterial and hemostasis environment. Synchronously and sustainably released SDF-1α and M2D-Exos from the HA@SDF-1α/M2D-Exos hydrogel enhanced osteogenesis and angiogenesis both in vivo and in vitro.

2.4. Hydrogel morphology test

The inner morphology of the HA-based hydrogel was explored by a desktop field emission scanning electron microscope (Model: Phenotype LE). The hydrogel sample was quickly frozen by immersing into liquid nitrogen and the frozen sample was cut into two pieces to expose the cross section of the hydrogel before lyophilization. The freeze-dried sample was observed with standard secondary electrons and at least three random regions were captured for analyzing.

2.5. Hydrogel rheological measurement

All the rheological characterization was tested by the rotary rheometer (Model: DHR 2; Manufacturer: Waters, USA) with 8 mm diameter parallel plates at room temperature. The gap size was always fixed at 0.2 mm. For the time sweep test, the frequency and strain were fixed at 1 Hz and 1%, respectively. For the strain sweep, the frequency was fixed at 1 Hz and the strain ranged from 1% to 1000%. For the shear-thinning test, the hydrogel was scanned with alternating high (300%) and low (1%) strain.

2.6. Biocompatibility and hemostatic assay

After administration of PBS or 4% HA hydrogel for 14 days, the major organs including the heart, liver, spleen, lung and kidney were collected, and processed for histology. Sections were stained with hematoxylin-eosin (H&E). The in vivo hemostatic assay of the hydrogel was evaluated using the hemorrhaging liver mouse model as previously described [21]. The antibacterial activity of the hydrogel surface against Gram-negative (*E. coli*, ATCC 8739) and Gram-positive bacteria (*S. aureus*, ATCC 29213; MRSA, ATCC BAA-40) was assessed. Briefly, 10 μL of bacterial suspension (10^6 CFU mL^{-1}, in PBS) was added to 990 μL PBS, 990 μL 4 μg/mL ampicillin (AM) solution or completely gelled hydrogel surface of different concentrations in a 48-well plate. After a 2 h incubation at 37 °C, the solution of each group was resuspended in PBS to 1 mL and plated on Luria-Bertani (LB) plate. The colony-forming units (CFU) were counted after incubation at 37 °C for 18 h and the results were expressed as bacterial viability %:

$$\textit{bacterial viability}\ \% = \frac{\text{survivor CFU on experiment group}}{\text{CFU of control}} \times 100$$

2.7. Cell culture and miRNA transfection

HMSC and HUVEC were donated by the Translational Research Laboratory, Union Hospital, Huazhong University of Science and Technology (China), and cultured in complete medium (#HUXMA-90011, Cyagen, USA) and RPMI 1640 (ThermoFisher Scientific) containing 10% FBS. AgomiR-5106 and antagomiR-5106 were synthesized by GenePharma (Shanghai, China), and transfected into HMSCs or HUVECs using Lipofectamine 3000 (ThermoFisher Scientific, MA, USA, #L3000001).

2.8. Exosome isolation from M2 and characterization

Bone marrow cells isolated from wild type C57BL/6J mice (male, 6 weeks old) were cultured in RPMI 1640 containing 10% FBS and 50 ng/mL Macrophage colony-stimulating factor (M-CSF, #216-MC, R&D System, Minneapolis, MN, USA) for 7 days to obtain bone marrow-derived macrophages (BMDMs), as previously described by our group [17]. Then 20 ng/mL IL-4 (#204-IL-010, R&D Systems) was added to the culture system for a further 24 h to obtain M2 macrophages. M2 macrophages were verified by flow cytometry (BD, LSRFortessa X-20, USA). And FITC anti-mouse F4/80 (#123107, Biolegend, USA), APC anti-mouse CD11b (#101212, Biolegend) and PE-cy7 anti-mouse CD206 (#141719, Biolegend) were used. After verification of the induction, the supernatant of M2s was collected and centrifuged at 1000 g for 10 min to remove debris and dead cells, followed by ultra-centrifugation for 6 h at 100,000g at 4 °C. The sediment was washed with PBS and centrifuged at 100,000g for 20 min to obtain the exosome pellet. BCA Protein Assay Kit (Beyotime, China), NanoFCM (High Sensitivity Flow Cytometry for Nanoparticle Analysis), western blotting and TEM (FEI Tecnai Spirit TEM 12) were used to analyze the quantification, global characterization and single characterization of exosomes. PKH 26 (#MINI26-1 KT, Sigma, MO, USA), FITC Phalloidin (#CA1620, Solarbio, China) and Hoechst 33342 (#G1127, Servicebio, China) were used to label the exosomes, F-actin, and nucleus, respectively, according to the manufacturer's instructions to visualize the uptake of M2D-Exos in HMSCs and HUVECs.

2.9. Exosome release assay

For exosome release assay, the HA@M2D-Exos hydrogel was obtained by mixing 50 μL 4% wt% HA-ADH with 5 μg M2D-Exos and 50 μL 4 wt% OHA-QA, shaken vigorously at 4 °C and then incubated at 37 °C. A Micro BCA Protein Assay Kit (ThermoFisher, USA) was used to assess the exosome release profile. In brief, 100 μL HA@M2D-Exos hydrogel were added to the upper 24-well Transwell plates (Corning, USA), while 500 μL PBS was placed in the lower chamber. Then 10 μL PBS was collected and replaced with fresh PBS at pre-determined time intervals to measure the exosome-release percentage.

2.10. SDF-1α release assay

FITC-labeled SDF-1α (FITC-SDF-1α) was used to replace SDF-1α to synthesize the HA@ FITC-SDF-1α hydrogel (with a final SDF-1α concentration of 500 ng/mL) in this assay. 1 mL PBS was added to a tube with 1 mL newly gelled HA@FITC-SDF-1α hydrogel followed by continuous shaking at a speed of 80 rpm/min at 37 °C. Then 300 μL of the medium was collected and replaced with fresh PBS at pre-determined time intervals. Fluorescence intensity was quantified with a Thermo Scientific Microplate Reader at λex = 495 nm and λem = 525 nm.

The remaining cell and animal experiments are described in the supplementary materials.

2.11. Statistical analysis

All data are presented as mean ± standard deviation (SD). Pair groups were assessed with Student's t-test, while multiple group comparisons were performed with a one-way analysis of variance (ANOVA) with Tukey's post hoc test. Significance was considered when $p < .05$. GraphPad Prism (V 7.0; GraphPad Software, Inc, La Jolla, CA) or R (V. 4.0.3) were used to perform the statistical analyses.

3. Results and discussion

3.1. The fabrication and characterization of the hydrogel

Fracture healing is an intricate biological process which requires interactions among cells in the periosteum, stem/progenitor cells, osteoblasts and other various cell types [22]. In this study, we designed an HA based hydrogel as the carrier for a protein growth factor and exosomes to promote angiogenesis and osteogenesis in an antibacterial microenvironment. In order to endow the hydrogel carrier with a convenient one-step injection property, we took advantage of the Schiff base interaction that occurs between an aldehyde group and hydrazide group and has a fast but mild reaction speed to provide our hydrogel a crosslinking formation ability. We firstly prepared two kinds of HA derivates, HA-ADH and OHA-QA (Fig. S1). As shown in Fig. 1a, HA-ADH solution and OHA-QA were loaded into a split compartment of a hand-made dual syringe. Then, the two solutions were mix-injected into

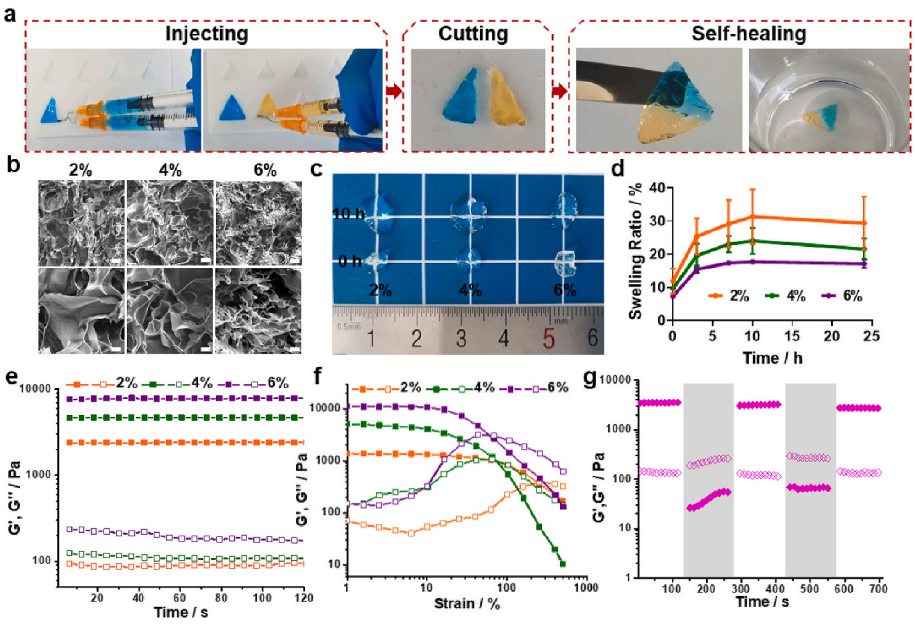

Fig. 1. (a) The HA-based hydrogel could be easily prepared through a one-step mixing-injection with a hand-made dual syringe. The hydrogel showed efficient self-recovery after being cut. (b) The SEM images of the HA-based hydrogel at different solid concentration. Scale bar: 100 μm (first line) and 30 μm (second line). (c) The photographs of HA-based hydrogel before and after reaching swelling equilibrium. (d) The swelling ratio curves for the HA-based hydrogel. Rheological (e) time sweep and (f) strain sweep of the HA-based hydrogel. (g) Time sweep testing of the HA-based hydrogel under alternating low/high strain (1%/300%). The shaded area represents the time sweep under high strain. Solid icon: storage modulus, hollow icon: loss modulus.

the triangle model at equal volumes. The hydrogel formed rapidly based on the hydrazone bond formation between the amino group of HA-ADH and the aldehyde group of OHA-QA as the crosslinker. Moreover, the HA based hydrogel also showed efficient self-healing properties. We cut two fresh HA-based hydrogels (one dyed blue and the other dyed yellow) in half. The cut hydrogel could be regenerated to a new one just through close contact with the hydrogel section for about 5 min. The recombined hydrogel could maintain its integrity long-term (even if immersed in water for 4 days, Fig. 1a). This satisfactory self-healing property can be attributed to the dynamic properties of the hydrazone group based on reversible crosslinking.

We then explored the property of HA-based hydrogel with different polymer content (2%, 4% and 6%). For example, 2% HA based hydrogel was formed by mix-injection of 2% HA-ADH solution and 2% OHA-QA solution. The SEM images clearly demonstrated the porous structure of the HA-based hydrogel and the pore size decreased with the increase of the polymer concentration (Fig. 1b). This interconnected porous structure could facilitate the substance exchange within and without the hydrogel to support cell growth. Consistent with previous research [23], despite increases of the concentration and decreases of porosity, HMSCs (were verified to have adipogenic, chondrogenic and osteogenic differentiation abilities in Fig. S2) and HUVECs maintained almost the same growth rate after being cultured with 2% or 4% hydrogels, while the proliferation rate of the two types of cells decreased significantly when the hydrogel concentration reached 6% (Fig. S3). We also tested the swelling ratio and swelling speed of our hydrogel (Fig. 1c and d). All three groups of HA-based hydrogel reached the swelling equilibrium after 10 h of PBS immersion. The swelling ratio of HA-based hydrogel was decreased with increase in polymer concentration, which was due to the reduced size of the nanopores inside the hydrogel. The polymer concentration of the HA-based hydrogel also effected their rheological mechanical properties. The time sweep results showed that the modulus of the HA-based hydrogel increased with an increase in the solid concentration (Fig. 1e). The susbequent strain sweep demonstrated that the breaking strain decreased from 259% to 63% when the solid concentration increased from 2% to 6% (Fig. 1f). This is because a higher solid concentration can lead to a denser hydrogel structure. Based on the above-mentioned observation, we selected the 4% group as the carrier for simulating cues, including protein growth factors and exosomes, as it had a moderate swelling ratio and rheological modulus. We then tested the hydrogel response to time sweep with cyclic low/high strain. Fig. 1g demonstrates that after breaking under high strain (300%), the HA-based hydrogel could recover to its initial solid state when the high strain was withdrawn. This showed the reversible crosslinking of the HA-based hydrogel, which is the foundation of its self-healing property. Moreover, our HA-based hydrogel also possessed good adhesion to the surface of different tissues, such as bone, skin, and the liver (Fig. S4). We speculated that this was due to the interaction between the native amino groups of tissue and the free aldehyde groups of the hydrogel. This good bio-adhesive property could help our HA-based hydrogel stay in the tissue defects after filling the defects by one-step injection to release its loaded simulating cues for a long time.

3.2. *Antibacterial function, biocompatibility and blood clotting ability of the HA hydrogel*

In terms of antibacterial activity, as shown in Fig. 2a, more than 95% of MRSA, and more than 99% of *S. aureus* and *E. coli* were eliminated when using the 4% HA hydrogel, while more than 99.9% of *S. aureus*, MRSA and *E. coli* were eliminated when using the 6% HA hydrogel. Therefore, both the 4% and 6% HA hydrogel had antibacterial functions. This efficient antibacterial property can be contributed to the positively charged quaternary ammonium groups in the main network of the HA hydrogel. These positively charged quaternary ammonium groups created a charged environment that is not conductive to bacterial growth, without affecting cell growth [24]. Based on the aforementioned results, 4% HA hydrogel was selected to perform subsequent experiments. After treatment with PBS or HA hydrogel for 14 days, the major organs (heart, liver, spleen, lung and kidney) were collected and stained with H&E. As shown in Fig. 2b, the HA hydrogel caused no appreciable abnormalities or damage to the organs when compared to the PBS group. And the proportions of live and dead cells of HMSCs and HUVECs were stable when treated with PBS, 2%, 4% or 6% hydrogel as assessed using an in vitro cytotoxicity assay (Fig. S5). This demonstrates that it is a relatively safe therapeutic material for fracture union. The hemostatic performance of the HA hydrogel was measured using a hemorrhaging liver mouse model. A significant difference in bleeding was seen between the HA hydrogel and control group at different time points (Fig. 2c). The amount of blood loss after 60 s of bleeding in the HA hydrogel group was also significantly lower than that of control group. Previous studies have demonstrated the positive charged quaternary ammonium groups were able to interact with the negative charged sites

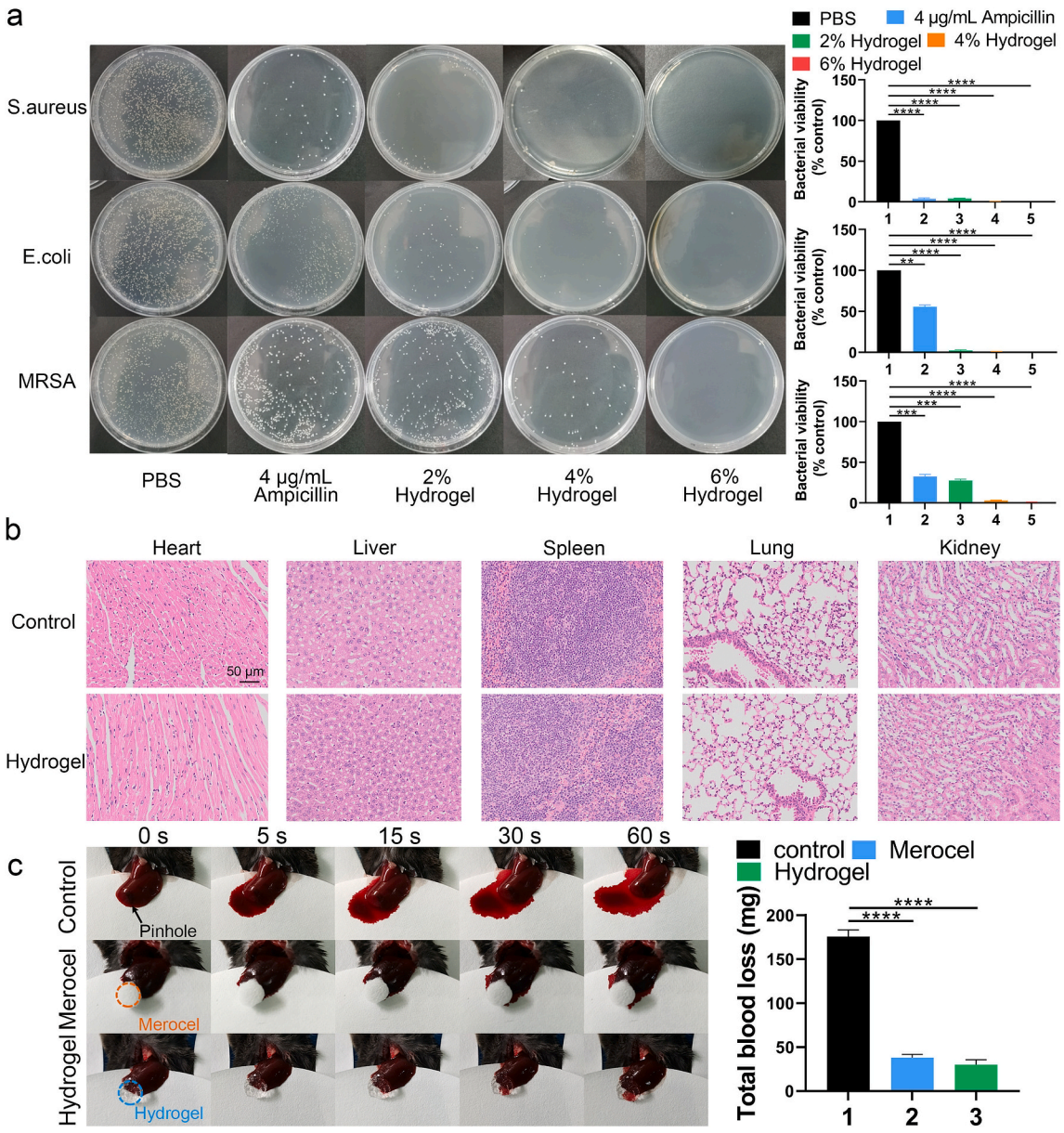

Fig. 2. Analysis of the antibacterial function, biocompatibility and blood clotting ability of the HA-based hydrogel. (a) Bacterial clones and bacteria viability % of *S. aureus*, *E. coli* and MRSA after planting and incubation for 18 h at 37 °C. (b) H&E staining of major organs (heart, liver, spleen, lung and kidney) after administration of PBS or the HA hydrogel for 14 days (scale bar = 50 μm). (c) Hemostatic assay using the hemorrhaging liver mouse model. Data are presented as mean ± SD of triplicate experiments, **P < .01, ***P < .001, ****P < .0001.

on the membranes of platelets to trigger the aggregation of the platelets [25,26]. Furthermore, our HA-hydrogel had a good swelling ratio to absorb liquid quickly. Therefore, we speculated that the quick hemostatic effect of our HA-based hydrogel could contributed to two factors: (1) the accelerated platelets aggregation induced by the negative charged quaternary ammonium; (2) the quick exudate absorption of fibrinogen and plasma proteins for further enhancing the platelets aggregation.

3.3. HA@SDF-1α hydrogel promotes migration of HMSCs and HUVECs

In order to enhance the chemotactic effect of the hydrogel in fracture repair, we added SDF-1α to the hydrogel and assessed its impact. Prior experiments identified that SDF-1 can promote BMSC migration in a dose-dependent manner when used in the range of 0–500 ng/mL. Co-assembling SDF-1 with bone morphogenetic protein 2 (BMP-2) at 500 ng/mL in a supramolecular hydrogel NapFFY promoted BMSC proliferation and migration both in vivo and in vitro [27]. Pre-diluted SDF-1α was mixed with 100 μL PBS at 4 °C to obtain different concentrations of the HA@SDF-1α hydrogel. As CXCR4 is downstream of SDF-1α and plays an important role in cell migration, we measured CXCR4 mRNA levels in the HMSCs and HUVECs seeded in complete medium or complete medium containing different concentrations of SDF-1α (Fig. 3a). CXCR4 protein expression was assessed with western blotting (WB, Fig. 3b). Overall, both 500 ng/mL and 600 ng/mL SDF-1α could induce an obvious enhanced CXCR4 level compared to other groups. Then HA@SDF-1α (500 ng/mL) hydrogel was selected for subsequent experiments. About 50% of SDF-1α was released within 72 h and the percentage of released SDF-1α reached 70% on day 7 (Fig. 3c). HMSCs and HUVECs were seeded in 6-well plates, HA hydrogel-coated 6-well plates or HA@SDF-1α hydrogel-coated plates. After 24 h of different treatments, cells were collected. A significantly higher expression of CXCR4 was observed in the HA@SDF-1α hydrogel group compared to the other groups as seen on qRT-PCR and western blotting

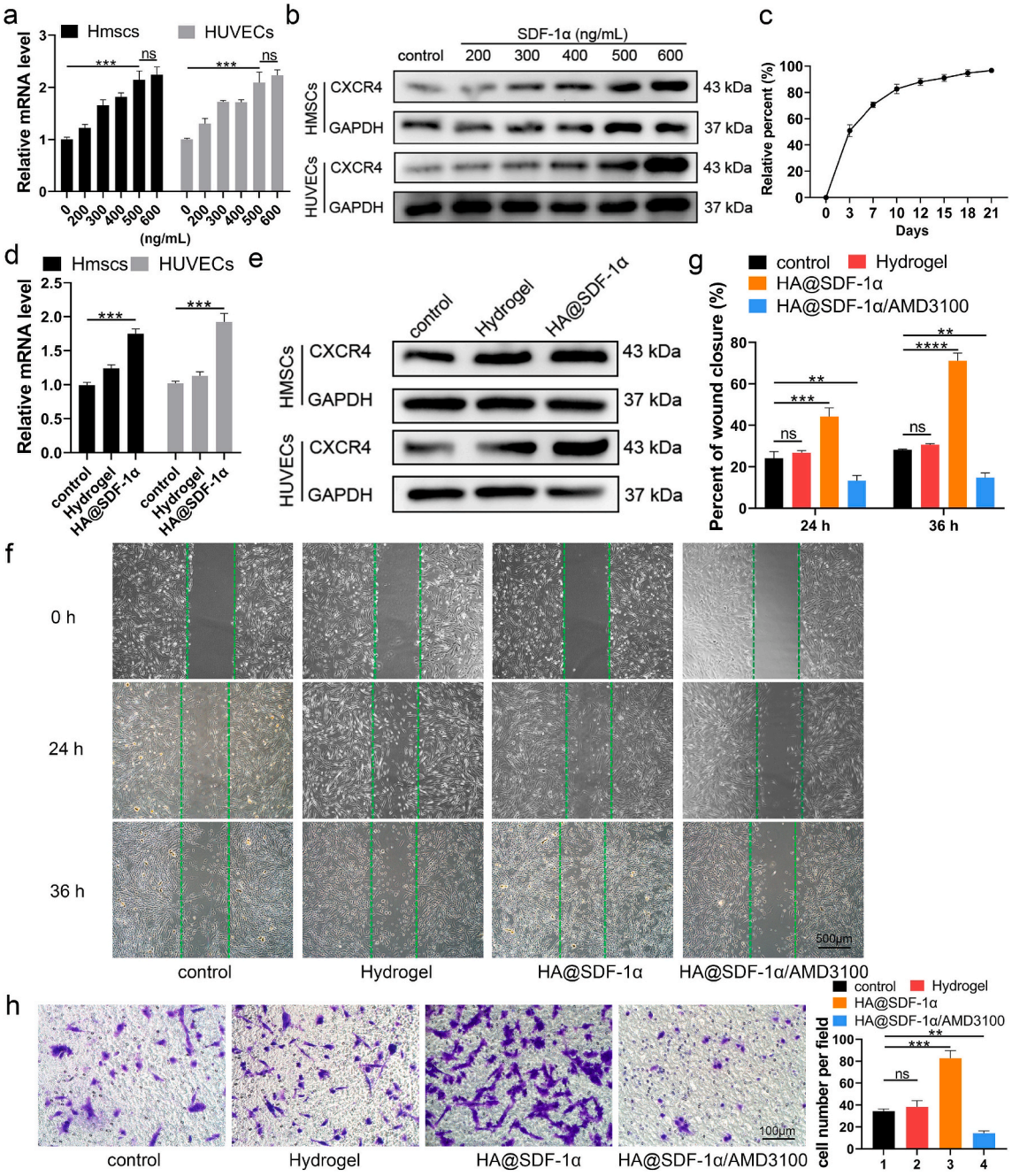

Fig. 3. The HA@SDF-1α hydrogel promoted chemotaxis of HMSCs and HUVECs. (a, b) SDF-1α stimulated a significant increase in the expression level of CXCR4 with increased SDF-1α concentration as verified with qRT-PCR analysis and western blotting. (c) SDF-1α could be released in a sustained manner. (d, e) qRT-PCR analysis and western blotting showed an enhanced expression level of CXCR4 when cells were cultured on an HA@SDF-1α hydrogel. (f–h) Scratch wound healing assay and transwell migration assay were conducted to test the migration effect of the HA@SDF-1α hydrogel (scale bar = 500 or 100 μm). Data are presented as mean ± SD of triplicate experiments, **P < .01, ***P < .001, ****P < .0001.

(Fig. 3d and e). Cells were replated in a hydrogel-free 6-well plate or 24-well Transwell plate to test the function of the HA@SDF-1α hydrogel on HMSCs and HUVECs. As shown, both HMSCs and HUVECs treated with HA@SDF-1α hydrogel exhibited higher rates of migration than cells in other groups, while theses effects could be abolished by 5 μg/mL AMD3100 (an SDF-1α/CXCR4 inhibitor; HMSCs: Fig. 3f–h; HUVECs: Fig. S6).

3.4. HA@M2D-exos hydrogel enhanced angiogenesis and osteogenesis in vitro

However, a delay in transforming the proinflammatory M1 phenotype to the anti-inflammatory M2 macrophages can limit inflammation resolution, resulting in chronic, delayed tissue repair [28,29]. Recent studies concluded that bone mimetic nano hydroxyapatite particles (BMnP) promoted M2 macrophage polarization and promoted osteogenesis in an IL-10-dependent manner [30]. Exosomes, which are secreted from various cell types, are 50–120 nm diameter extracellular vesicles carrying a variety of bioactive substances, including noncoding RNA, mRNA, DNA, proteins and other molecules [31]. The role of macrophage-derived exosomes in fracture healing has become a popular research endeavor [32,33]. M2D-Exos could be transferred to BMSCs to accelerate osteoblast differentiation [17]. First, isolated M2 macrophages were induced by IL-4 and identified via flow cytometry

(Fig. S7a). A sample of M2D-Exos were isolated from 50 mL M2 macrophage cell supernatant and the isolated M2D-Exos were about 20 μg in 50 μL (particle number: 2.01 × 10^{10} particle/mL).Then the M2D-Exos were isolated and photographed with a transmission electron microscope (TEM; Fig. S7b). Consistent with published results on exosomes [34], the NanoSight analysis showed a 50–150 nm range size of M2D-Exos (Fig. S7c). NaonoFCM results showed that M2D-Exos presented CD9, CD63 and CD81 when compared to control sample (Fig. S7e). Western blot analysis showed that M2D-Exos samples had a higher expression of tumor susceptibility gene 101 protein (TSG101), but did not contain calnexin (Fig. S7e). HMSCs and HUVECs were seeded to PKH-26-labeled HA@M2D-Exos hydrogel coated confocal dishes, and it was shown that M2D-Exos could be successfully transferred into cells (Fig. S7f).

In order to further investigate the function of M2D-Exos in fracture healing, firstly we mixed 0.5, 1, 5 or 10 μg M2D-Exos respectively with 100 μL HA hydrogel at 4 °C to obtain HA@M2D-Exos hydrogel to measure the dose depend effect of M2D-Exos. CCK-8 results showed that

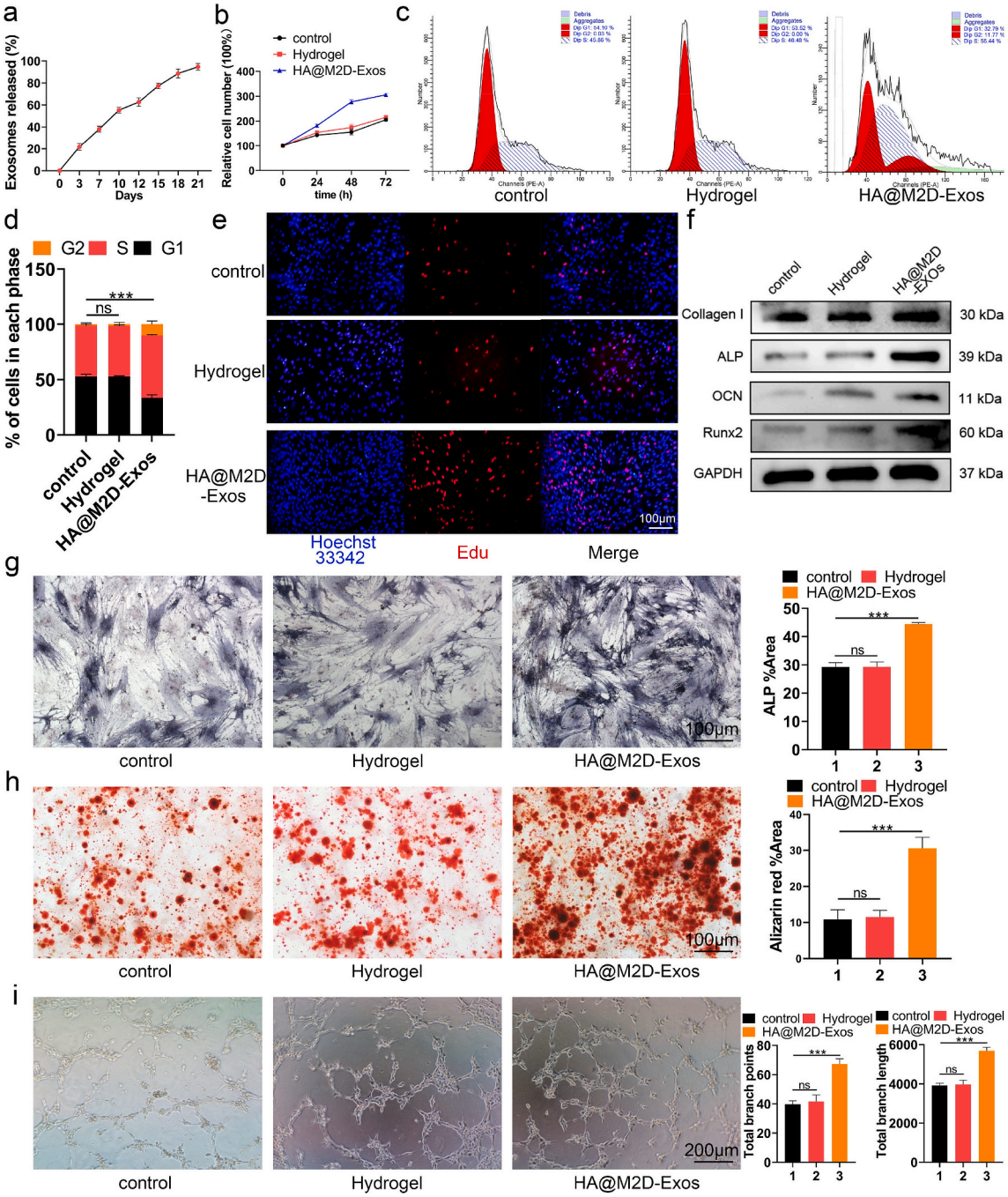

Fig. 4. The HA@M2D-Exos hydrogel enhanced the function of HMSCs and HUVECs. (a) M2D-Exos could be released in a sustained manner. (b, e) HMSCs were treated with PBS, HA hydrogel or HA@M2D-Exos hydrogel for 48 h. The effect of HA@M2D-Exos hydrogel on HMSCs proliferation was assessed with CCK-8 and EdU assays (scale bar = 100 μm). (c, d) Compared to the control, more cells progressed to the S phase after treatment with the HA@M2D-Exos hydrogel as measured with flow cytometry. (f) Osteogenic gene expression level was measured in each group with western blotting. (g) ALP staining of treated HMSCs after osteogenic induction for a week (scale bar = 100 μm). (h) Alizarin Red staining of treated HMSCs after osteogenic induction for three weeks (scale bar = 100 μm). (i) Tube formation assay of HUVECs following different treatments (scale bar = 200 μm). Data are presented as mean ± SD of triplicate experiments, **P < .01, ***P < .001.

both 5 μg and 10 μg M2D-Exos significantly enhanced the proliferation of both HMSCs and HUVECs, however, no significant difference was found between these two groups (Fig. S8). Therefore, we mixed 5 μg of M2D-Exos per 100 μL HA hydrogel to form HA@M2D-Exos hydrogel for the subsequent experiments. Confocal results showed that PKH-26 labeled M2D-Exos could be evenly distributed in the hydrogel, maintaining the original shape (Fig. S9). Then an exosome release assay showed that 21.7% M2D-Exos were released in the first 72 h, while the remaining 40% of M2D-Exos were released ten days later, demonstrating a long-term effect of M2D-Exos in vitro (Fig. 4a). Then CCK-8, cell cycle assay and EdU assay were conducted to test the effect of HA@M2D-Exos hydrogel on HMSC and HUVEC proliferation. As shown, HMSCs and HUVECs treated with HA@M2D-Exos hydrogel had a higher relative cell number, larger percentage of S phase and higher 5-ethynyl-2' -deoxyuridine (EdU) -positive cell numbers (HMSCs: Fig. 4b–e, quantitative analysis of EdU assay for HMSCs: Fig. S10a, HUVECs: Figs. S10b–S10f). Osteogenic related genes, including collagen I, alkaline phosphatase (ALP), osteocalcin (OCN), and Runt-related transcription factor 2 (Runx2), were assessed with western blotting in the HMSC, and a positive effect of the HA@M2D-Exos hydrogel on osteogenic

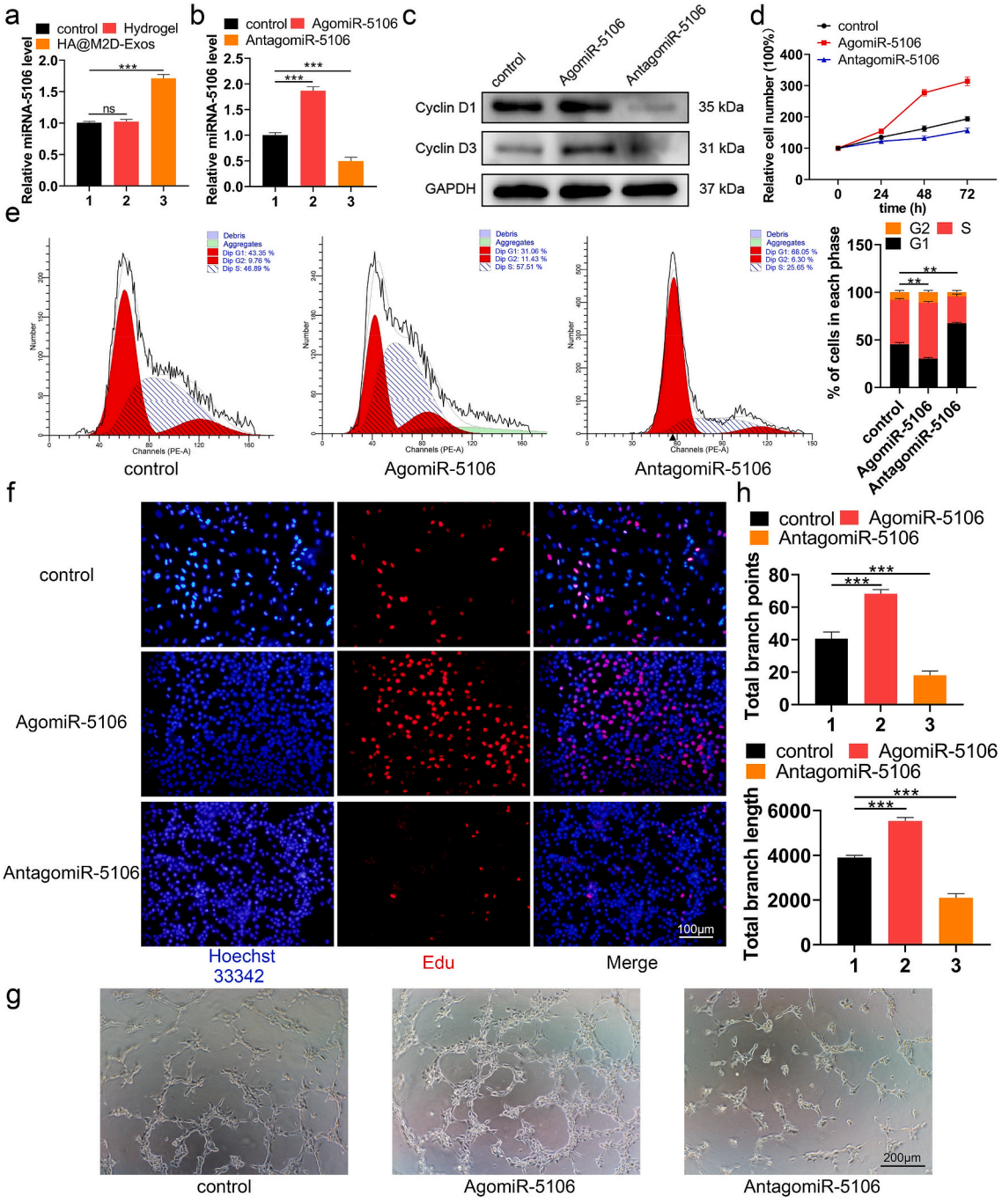

Fig. 5. M2D-Exosomal miRNA-5106 enhanced angiogenesis in vitro. (a) The miR-5106 level was significantly higher after HA@M2D-Exos hydrogel treatment. (b) HUVECs were treated with PBS or transfected with AgomiR-5106 or AntagomiR-5106. The miR-5106 expression level was assessed using qRT-PCR analysis. (c) Proliferation-related protein Cyclin D1 and Cyclin D3 level were assessed with western blotting. (d, f) The effect of miR-5106 on HUVEC proliferation was assessed with CCK-8 and EdU assay (scale bar = 100 μm). (e) The proliferation state was assessed with a cell cycle assay. (g, h) HUVEC tube formation ability was significantly higher after miR-5106 transfection (scale bar = 200 μm). Data are presented as mean ± SD of triplicate experiments, **P < .01, ***P < .001.

differentiation was identified (Fig. 4f). ALP activity and mineral deposition were also enhanced after treatment with the HA@M2D-Exos hydrogel (Fig. 4g and h). Furthermore, HA@M2D-Exos hydrogel induced tube formation in the HUVEC (Fig. 4i). However, HA@M2D-Exos hydrogel did not enhance migration ability of HMSCs or HUVECs through scratch wound healing assay and transwell migration assay (Fig. S11).

3.5. HA@M2D-exos hydrogel-derived miRNA-5106 enhanced angiogenesis in vitro

MicroRNAs (miRNAs) are evolutionally conserved, single-stranded noncoding RNAs that are approximately 23 nucleotides in length and are involved in posttranscriptional gene expression. Multiple articles have reported a link between miRNAs and bone repair [35,36]. We have previously shown with microarray analysis that miR-5106 is highly

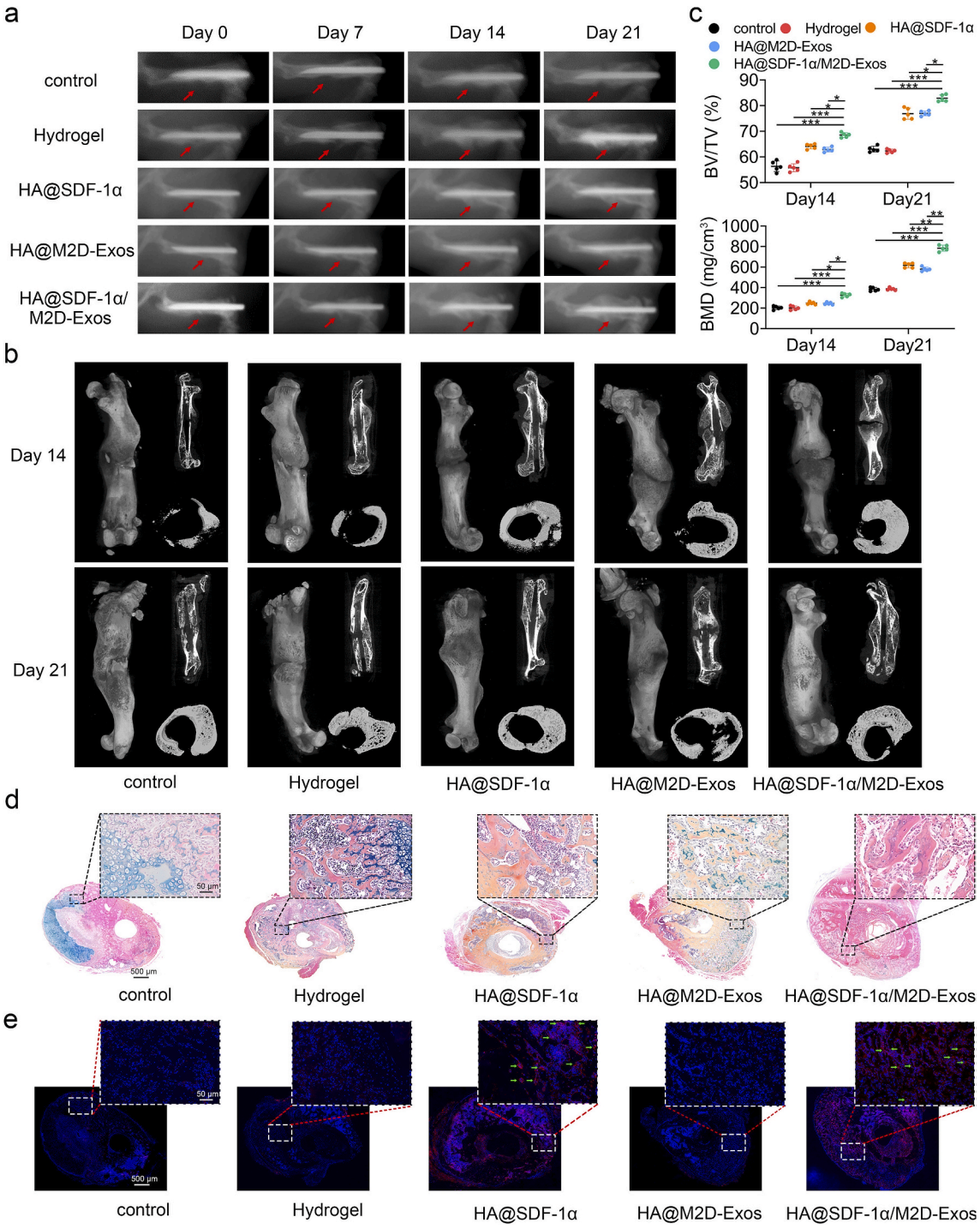

Fig. 6. The HA@SDF-1α/M2D-Exos hydrogel promoted osteogenesis in vivo. (a) X-ray comparison of the fracture healing process of the control, hydrogel, HA@SDF-1α hydrogel, HA@M2D-Exos hydrogel and HA@SDF-1α/M2D-Exos hydrogel groups on day 7, 14 and day 21 post-injury. (b) micro-CT 3D construction, longitudinal sections and cross sectional images on post-fracture day 14 and 21. (c) Statistical results of BV/TV and BMD. (d) Alcian Blue/HE/orange G staining was conducted to show the bone and cartilage area in each group. (e) SDF-1 α immunofluorescence assay was conducted to show the distribution of SDF-1 α in the fracture site (scale bar = 50 μm/500 μm). Green arrows showed SDF-1α+ cells. N = 5 mice/group, data are presented as mean ± SD, *P < .05, **P < .01, ***P < .001.

enriched in M2D-Exos and plays an indispensable role in osteogenesis, both in vivo and in vitro [17]. As no prior literature has studied the role of miR-5106 in angiogenesis, we sought to investigate the effect of HA@M2D-Exos hydrogel-derived miR-5106 on angiogenesis. The miR-5106 level was significantly higher in the HA@M2D-Exos hydrogel group compared to the HA hydrogel group (Fig. 5a). Therefore, we transfected AgomiR-5106 and AntagomiR-5106 into HUVECs and measured the miR-5106 level (Fig. 5b). Treated cells were collected for western blotting, and a higher expression of Cyclin D1 and Cyclin D3 protein was seen in the AgomiR-5106 group (Fig. 5c). CCK-8, cell cycle assay and an EdU assay showed that miR-5106 promoted the proliferation of HUVECs (Fig. 5d–f, quantitative analysis of EdU assay: Fig. S12a). Transfecting cells with miR-5106 enhanced the tube formation ability of HUVECs (Fig. 5g and h). Furthermore, when transfected with antagomiR-5106 supplemented with M2D-Exos, tube formation ability of HUVECs impaired significantly when compared to M2D-Exos group (Fig. S12b). Therefore, except for the osteoblast differentiation function shown with the WB, ALP staining as well as Alizarin Red staining [17], M2 derived exosomal miR-5106 was also able to promote angiogenesis of HUVECs as shown with flow cytometry, EdU staining and tube forming experiments. As for the downstream of miR-5106, since miR-5106 is highly enriched in M2D-Exos, and could be transferred to BMSCs wherein it targets SIK2 and SIK3 genes to promote osteoblast differentiation [17]. The degradation of SIK2 protein concomitantly with the dephosphorylation of the CREB-specific coactivator transducer of regulated CREB activity 1 (TORC1), resulting in the activation of CREB and its downstream gene targets [37,38]. Additionally, CREB activation induces angiogenesis in vitro, depending on the EZH2/TSP1 axis [39]. Therefore, we could suppose that M2 derived exosomal miR-5106 may inhibit the expression of SIK2 and promote angiogenesis through activating CREB signaling pathway. Furthermore, M2D-Exos was also reported to reduce adipogenesis of BMSCs through the miR-690/IRS-1/TAZ axis [40]. In conclusion, M2D-Exos have great application potential in promoting bone repair.

3.6. HA@ SDF-1α/M2D-exos hydrogel enhanced angiogenesis and osteogenesis in vivo

In order to promote infiltration of HMSCs and HUVECs and maximize osteogenesis and angiogenesis function in vivo, we mixed 100 μL HA hydrogel with 1 μg of SDF-1α and 100 μg of M2D-Exos to obtain an HA@ SDF-1α/M2D-Exos hydrogel. We administrated 100 μL DiR-labeled HA@ SDF-1α/DiR-M2D-Exos at the fracture site after injury, and small animal imaging proved that M2D-Exos could be released in a sustained manner at the fracture site during the fracture healing process (Fig. S13). Then we administered 100 μL PBS, HA hydrogel, HA@SDF-1α hydrogel, HA@M2D-Exos hydrogel or HA@SDF-1α/M2D-Exos hydrogel directly to the murine fracture site on day 0 post-surgery. Imaging, including X-ray and micro-CT, showed a significantly reduced fracture gap and a larger callus volume in the HA@ SDF-1α/M2D-Exos hydrogel group (Fig. 6a and b). Bone indices, including bone volume (BV), trabecula volume (TV), BV/TV, and bone mineral density (BMD) were consistent with the aforementioned results (Fig. 6c, Fig. S14a). Murine femurs were collected for histological analysis. Alcian Blue/HE/orange G staining, Masson Trichrome and Safranin O/Fast Green stain showed that the HA@ SDF-1α/M2D-Exos hydrogel treatment increased bone and decreased cartilage both on day 14 and day 21 post-injury (Fig. 6d, Figs. S14b–S14d). The distribution of SDF-1α at the fracture site of each group was shown with SDF-1α immunofluorescence. It was shown that the fluorescence intensity of SDF-1α increased significantly after injection of SDF-loaded HA hydrogel (Fig. 6e, Fig. S14e). For analysis of the angiogenic ability of the HA@ SDF-1α/M2D-Exos hydrogel, treated mice were anesthetized for early blood flow assessment of the fracture site on day 10 post-injury (Fig. 7a). CD31 immunohistochemistry (IHC) staining and Endomucin (EMCN) immunofluorescence staining were conducted on day 21 post-surgery to assess the mid-late blood flow condition of each group. (Fig. 7b, c, Fig. S10f). HA@SDF-1α/M2D-Exos hydrogel displayed the greatest promoting effect on angiogenesis in vivo.

Traditional strategies focus on the morphological features of the scaffold, including porosity and pore size, to promote osteogenesis [41] or maximize the biocompatibility and efficacy of loaded cell and growth

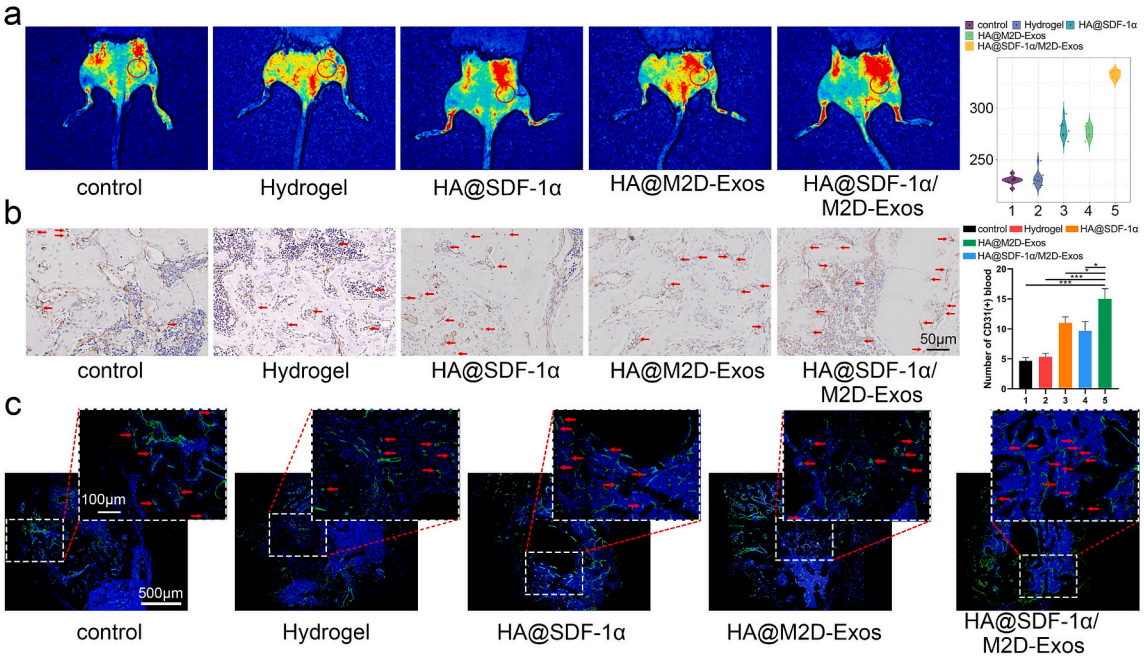

Fig. 7. HA@SDF-1α/M2D-Exos hydrogel promoted angiogenesis in vivo. Mice were treated with PBS, HA hydrogel, HA@SDF-1α hydrogel, HA@M2D-Exos hydrogel or HA@SDF-1α/M2D-Exos hydrogel. (a) Blood flow level was assessed with LSCI imaging. (b, c) CD31 immunohistochemistry (scale bar = 50 μm) and EMCN immunofluorescence assay (scale bar = 100 μm/500 μm) were conducted to show the extent of vascularization of each group. Red arrows show $CD31^+$ or EMCN + cells. N = 5 mice/group, data are presented as mean ± SD, **P < .01, ***P < .001.

factor delivery to enhance application in the clinic [42]. Controlled local multiple growth factor delivery has become a promising strategy for both bone regeneration and vascular growth, however, it is still controversial whether VEGF and BMP-2, the most representative growth factors in these two aspects, have synergistic effects in composite bone-muscle injury [43,44]. Targeted delivery of osteo-inductive factors or small molecule drugs, such as resveratrol and strontium ranelate, is also a promising scheme to design osteogenic biomaterials. However, these drugs are often not naturally produced during the fracture healing process, and their introduction requires strict biosafety evaluation and dose effect evaluation [45,46]. The locally injectable HA@SDF-1α/M2D-Exos hydrogel presented in this research was compatibly with the natural healing process of fractures and had a beneficial effect on bone repair through eradication of bacterial infection, and promotion of osteogenesis and angiogenesis.

The limitations of this work should be mentioned. First, M2D-Exos were added to the HA hydrogel, focus was placed on their effects on osteogenesis and angiogenesis. We did not study whether the HA@M2D-Exos hydrogel could locally promote M1 to M2 phenotype switching. This is a future research priority. Second, we did not assess the effects on the migration of MSC and endothelial cells following in vivo local treatment with the HA@SDF-1α/M2D-Exos hydrogel at the femoral fracture site. This will be assessed in future research. Finally, at this stage, the clinical application of HA@SDF-1α/M2D-Exos hydrogel on fracture healing has not yet been assessed.

4. Conclusion

In this research, we showed that a novel HA@SDF-1α/M2D-Exos hydrogel provided local antibacterial activity, recruited and promoted the proliferation of HMSCs and HUVECs, stimulated extracellular matrix mineralization and HUVEC tube formation, enhanced osteogenesis and angiogenesis both in vivo and in vitro, and ultimately contributed to improved fracture healing. Collectively, the locally injectable HA@SDF-1α/M2D-Exos hydrogel presented in this research was compatibly with the natural healing process of fractures and had a beneficial effect on bone repair through eradication of bacterial infection, and promotion of osteogenesis and angiogenesis.

CRediT authorship contribution statement

Lang Chen: Conceptualization, Methodology, Software, Investigation, Data curation, Writing – original draft. **Chenyan Yu:** Validation, Formal analysis, Data curation. **Yuan Xiong:** Conceptualization, Methodology, Resources. **Kai Chen:** Investigation, Data curation, Formal analysis. **Pei Liu:** Validation, Writing – original draft. **Adriana C. Panayi:** Writing – review & editing. **Xiufeng Xiao:** Visualization, Funding acquisition. **Qian Feng:** Writing – review & editing, Supervision, Funding acquisition. **Bobin Mi:** Resources, Supervision, Project administration. **Guohui Liu:** Conceptualization, Investigation, Supervision, Funding acquisition.

Declaration of competing interest

The authors declare that they have no known competing financial interests or personal relationships that could have appeared to influence the work reported in this paper.

Acknowledgements

This study was supported by the National Natural Science Foundation of China (grant No. 82002313, 82072444and 31900963), the National Key Research and Development Program of China (grants No. 2018YFC2001502and 2018YFB1105705), the Fundamental Research Funds for the Central Universities (HUST: 2021yjsCXCY124; FNU: 2021CDJQY-017) and the Health-Education Joint Research Project of Fujian Province (2019-WJ-22). Thanks for the technical support by the Huazhong University of Science & Technology Analytical & Testing center, Medical sub-center.

Appendix A. Supplementary data

Supplementary data to this article can be found online at https://doi.org/10.1016/j.bioactmat.2022.07.030.

References

[1] J.J. Nielsen, S.A. Low, N.T. Ramseier, R.v. Hadap, N.A. Young, M. Wang, P.S. Low, Analysis of the bone fracture targeting properties of osteotropic ligands, J. Contr. Release 329 (2021) 570–584, https://doi.org/10.1016/j.jconrel.2020.09.047.
[2] G.B. Reahl, L. Gerstenfeld, M. Kain, Orthopedic management of fractures (M kacena and L gerstenfeld, section editors), Epidemiology, Clinical Assessments, and Current Treatments of Nonunions (1914), https://doi.org/10.1007/s11914-020-00575-6.
[3] L. Johnson, E. Igoe, G. Kleftouris, I. v Papachristos, C. Papakostidis, P. v Giannoudis, Physical Health and psychological outcomes in adult patients with long-bone fracture non-unions: evidence today, J. Clin. Med. 8 (2019), https://doi.org/10.3390/jcm8111998.
[4] P. Qiu, M. Li, K. Chen, B. Fang, P. Chen, Z. Tang, X. Lin, S. Fan, Periosteal matrix-derived hydrogel promotes bone repair through an early immune regulation coupled with enhanced angio- and osteogenesis, Biomaterials 227 (2020), https://doi.org/10.1016/j.biomaterials.2019.119552.
[5] X. Zhang, P. Huang, G. Jiang, M. Zhang, F. Yu, X. Dong, L. Wang, Y. Chen, W. Zhang, Y. Qi, W. Li, H. Zeng, A novel magnesium ion-incorporating dual-crosslinked hydrogel to improve bone scaffold-mediated osteogenesis and angiogenesis, Mater. Sci. Eng. C 121 (2021), https://doi.org/10.1016/j.msec.2021.111868.
[6] T.A. Einhorn, L.C. Gerstenfeld, Fracture healing: mechanisms and interventions, Nat. Rev. Rheumatol. 11 (2015) 45–54, https://doi.org/10.1038/nrrheum.2014.164.
[7] L. Claes, S. Recknagel, A. Ignatius, Fracture healing under healthy and inflammatory conditions, Nat. Rev. Rheumatol. 8 (2012) 133–143, https://doi.org/10.1038/nrrheum.2012.1.
[8] P. Su, Y. Tian, C. Yang, X. Ma, X. Wang, J. Pei, A. Qian, Mesenchymal stem cell migration during bone formation and bone diseases therapy, Int. J. Mol. Sci. 19 (2018), https://doi.org/10.3390/ijms19082343.
[9] J. Pajarinen, T. Lin, E. Gibon, Y. Kohno, M. Maruyama, K. Nathan, L. Lu, Z. Yao, S. B. Goodman, Mesenchymal stem cell-macrophage crosstalk and bone healing, Biomaterials 196 (2019) 80–89, https://doi.org/10.1016/j.biomaterials.2017.12.025.
[10] A. Mantovani, A. Sica, S. Sozzani, P. Allavena, A. Vecchi, M. Locati, The chemokine system in diverse forms of macrophage activation and polarization, Trends Immunol. 25 (2004) 677–686, https://doi.org/10.1016/j.it.2004.09.015.
[11] J. Ringe, S. Strassburg, K. Neumann, M. Endres, M. Notter, G.-R. Burmester, C. Kaps, M. Sittinger, Towards in situ tissue repair: human mesenchymal stem cells express chemokine receptors CXCR1, CXCR2 and CCR2, and migrate upon stimulation with CXCL8 but not CCL2, J. Cell. Biochem. 101 (2007) 135–146, https://doi.org/10.1002/jcb.21172.
[12] J.-M. Tang, J.-N. Wang, L. Zhang, F. Zheng, J.-Y. Yang, X. Kong, L.-Y. Guo, L. Chen, Y.-Z. Huang, Y. Wan, S.-Y. Chen, VEGF/SDF-1 promotes cardiac stem cell mobilization and myocardial repair in the infarcted heart, Cardiovasc. Res. 91 (2011) 402–411, https://doi.org/10.1093/cvr/cvr053.
[13] S.K. Ghadge, S. Mühlstedt, C. Özcelik, M. Bader, SDF-1α as a therapeutic stem cell homing factor in myocardial infarction, Pharmacol. Ther. 129 (2011) 97–108, https://doi.org/10.1016/j.pharmthera.2010.09.011.
[14] Q. Chen, C. Zheng, Y. Li, S. Bian, H. Pan, X. Zhao, W.W. Lu, Bone targeted delivery of SDF-1 via alendronate functionalized nanoparticles in guiding stem cell migration, ACS Appl. Mater. Interfaces 10 (2018) 23700–23710, https://doi.org/10.1021/acsami.8b08606.
[15] M. S, J. H, S. Rj, Exosomes: extracellular organelles important in intercellular communication, J. Proteonomics 73 (2010) 1907–1920, https://doi.org/10.1016/J.JPROT.2010.06.006.
[16] Y. Hu, X. Li, Q. Zhang, Z. Gu, Y. Luo, J. Guo, X. Wang, Y. Jing, X. Chen, J. Su, Exosome-guided bone targeted delivery of Antagomir-188 as an anabolic therapy for bone loss, Bioact. Mater. 6 (2021) 2905–2913, https://doi.org/10.1016/j.bioactmat.2021.02.014.
[17] Y. Xiong, L. Chen, C. Yan, W. Zhou, T. Yu, Y. Sun, F. Cao, H. Xue, Y. Hu, D. Chen, B. Mi, G. Liu, M2 Macrophagy-derived exosomal miRNA-5106 induces bone mesenchymal stem cells towards osteoblastic fate by targeting salt-inducible kinase 2 and 3, J. Nanobiotechnol. 18 (2020), https://doi.org/10.1186/s12951-020-00622-5.
[18] X. Bai, M. Gao, S. Syed, J. Zhuang, X. Xu, X.Q. Zhang, Bioactive hydrogels for bone regeneration, Bioact. Mater. 3 (2018) 401–417, https://doi.org/10.1016/j.bioactmat.2018.05.006.
[19] X. Ji, X. Yuan, L. Ma, B. Bi, H. Zhu, Z. Lei, W. Liu, H.X. Pu, J. Jiang, X. Jiang, Y. Zhang, J. Xiao, Mesenchymal stem cell-loaded thermosensitive hydroxypropyl chitin hydrogel combined with a three-dimensional-printed poly(ε-caprolactone)/nano-hydroxyapatite scaffold to repair bone defects via osteogenesis, angiogenesis

and immunomodulation, Theranostics 10 (2020) 725–740, https://doi.org/10.7150/thno.39167.
[20] X. Ji, X. Yuan, L. Ma, B. Bi, H. Zhu, Z. Lei, W. Liu, H. Pu, J. Jiang, X. Jiang, Y. Zhang, J. Xiao, Mesenchymal stem cell-loaded thermosensitive hydroxypropyl chitin hydrogel combined with a three-dimensional-printed poly(ε-caprolactone)/nano-hydroxyapatite scaffold to repair bone defects via osteogenesis, angiogenesis and immunomodulation, Theranostics 10 (2020) 725–740, https://doi.org/10.7150/thno.39167.
[21] X. Pan, D. Kong, W. Wang, W. Liu, W. Ou-Yang, C. Zhang, Q. Wang, P. Huang, C. Zhang, Y. Li, Synthetic polymeric antibacterial hydrogel for methicillin-resistant staphylococcus aureus-infected wound healing: nanoantimicrobial self-assembly, drug- and cytokine-free strategy, ACS Nano 14 (2020) 12905–12917, https://doi.org/10.1021/acsnano.0c03855.
[22] K. Hankenson, G. Zmmerman, R. Marcucio, Biological perspectives of delayed fracture healing, Injury 45 (2014) S8, https://doi.org/10.1016/J.INJURY.2014.04.003.
[23] Y. Xu, J. Zhou, C. Liu, S. Zhang, F. Gao, W. Guo, X. Sun, C. Zhang, H. Li, Z. Rao, S. Qiu, Q. Zhu, X. Liu, X. Guo, Z. Shao, Y. Bai, X. Zhang, D. Quan, Understanding the role of tissue-specific decellularized spinal cord matrix hydrogel for neural stem/progenitor cell microenvironment reconstruction and spinal cord injury, Biomaterials 268 (2021), 120596, https://doi.org/10.1016/j.biomaterials.2020.120596.
[24] Z. Yang, R. Huang, B. Zheng, W. Guo, C. Li, W. He, Y. Wei, Y. Du, H. Wang, D. Wu, H. Wang, Highly stretchable, adhesive, biocompatible, and antibacterial hydrogel dressings for wound healing, Adv. Sci. 8 (2021), 2003627, https://doi.org/10.1002/advs.202003627.
[25] M. Yin, Y. Wang, Y. Zhang, X. Ren, Y. Qiu, T.-S. Huang, Novel quaternarized N-halamine chitosan and polyvinyl alcohol nanofibrous membranes as hemostatic materials with excellent antibacterial properties, Carbohydr. Polym. 232 (2020), 115823, https://doi.org/10.1016/j.carbpol.2019.115823.
[26] J. Wen, M. Weinhart, B. Lai, J. Kizhakkedathu, D.E. Brooks, Reversible hemostatic properties of sulfabetaine/quaternary ammonium modified hyperbranched polyglycerol, Biomaterials 86 (2016) 42–55, https://doi.org/10.1016/j.biomaterials.2016.01.067.
[27] J. Tan, M. Zhang, Z. Hai, C. Wu, J. Lin, W. Kuang, H. Tang, Y. Huang, X. Chen, G. Liang, Sustained release of two bioactive factors from supramolecular hydrogel promotes periodontal bone regeneration, ACS Nano 13 (2019) 5616–5622, https://doi.org/10.1021/acsnano.9b00788.
[28] J. Lee, H. Byun, S.K. Madhurakkat Perikamana, S. Lee, H. Shin, Current advances in immunomodulatory biomaterials for bone regeneration, Adv. Healthcare Mater. 8 (2019), https://doi.org/10.1002/adhm.201801106.
[29] G.C. Gurtner, S. Werner, Y. Barrandon, M.T. Longaker, Wound repair and regeneration, Nature 453 (2008) 314–321, https://doi.org/10.1038/nature07039.
[30] O.R. Mahon, D.C. Browe, T. Gonzalez-Fernandez, P. Pitacco, I.T. Whelan, S. von Euw, C. Hobbs, V. Nicolosi, K.T. Cunningham, K.H.G. Mills, D.J. Kelly, A. Dunne, Nano-particle mediated M2 macrophage polarization enhances bone formation and MSC osteogenesis in an IL-10 dependent manner, Biomaterials 239 (2020), https://doi.org/10.1016/j.biomaterials.2020.119833.
[31] D.M. Pegtel, S.J. Gould, Exosomes, Annual Review of Biochemistry 88 (2019) 487–514, https://doi.org/10.1146/annurev-biochem-013118-111902.
[32] D. Wang, J. Wang, J. Zhou, X. Zheng, The role of adenosine receptor A2A in the regulation of macrophage exosomes and vascular endothelial cells during bone healing, J. Inflamm. Res. 14 (2021) 4001–4017, https://doi.org/10.2147/jir.s324232.
[33] D. Zhang, Y. Wu, Z. Li, H. Chen, S. Huang, C. Jian, A. Yu, MiR-144-5p, an exosomal miRNA from bone marrow-derived macrophage in type 2 diabetes, impairs bone fracture healing via targeting Smad1, J. Nanobiotechnol. 19 (2021), https://doi.org/10.1186/s12951-021-00964-8.
[34] J. Fan, C.S. Lee, S. Kim, C. Chen, T. Aghaloo, M. Lee, Generation of small RNA-modulated exosome mimetics for bone regeneration, ACS Nano 14 (2020) 11973–11984, https://doi.org/10.1021/acsnano.0c05122.
[35] L. Chen, Y. Xiong, C. Yan, W. Zhou, Y. Endo, H. Xue, Y. Hu, L. Hu, X. Leng, J. Liu, Z. Lin, B. Mi, G. Liu, LncRNA KCNQ1OT1 accelerates fracture healing via modulating miR-701-3p/FGFR3 axis, Faseb. J. 34 (2020) 5208–5222, https://doi.org/10.1096/fj.201901864RR.
[36] T. Xu, Y. Luo, J. Wang, N. Zhang, C. Gu, L. Li, D. Qian, W. Cai, J. Fan, G. Yin, Exosomal miRNA-128-3p from mesenchymal stem cells of aged rats regulates osteogenesis and bone fracture healing by targeting Smad5, J. Nanobiotechnol. 18 (2020), https://doi.org/10.1186/s12951-020-00601-w.
[37] N.J. Darling, P. Cohen, Nuts and bolts of the salt-inducible kinases (SIKs), Biochem. J. 478 (2021) 1377–1397, https://doi.org/10.1042/BCJ20200502.
[38] T. Sasaki, H. Takemori, Y. Yagita, Y. Terasaki, T. Uebi, N. Horike, H. Takagi, T. Susumu, H. Teraoka, K. Kusano, O. Hatano, N. Oyama, Y. Sugiyama, S. Sakoda, K. Kitagawa, SIK2 is a Key regulator for neuronal survival after ischemia via TORC1-CREB, Neuron 69 (2011) 106–119, https://doi.org/10.1016/j.neuron.2010.12.004.
[39] Y. Zhang, D. Zheng, T. Zhou, H. Song, M. Hulsurkar, N. Su, Y. Liu, Z. Wang, L. Shao, M. Ittmann, M. Gleave, H. Han, F. Xu, W. Liao, H. Wang, W. Li, Androgen deprivation promotes neuroendocrine differentiation and angiogenesis through CREB-EZH2-TSP1 pathway in prostate cancers, Nat. Commun. 9 (2018) 4080, https://doi.org/10.1038/s41467-018-06177-2.
[40] Z. Li, Y. Wang, S. Li, Y. Li, Exosomes derived from M2 macrophages facilitate osteogenesis and reduce adipogenesis of BMSCs, Front. Endocrinol. 12 (2021), 680328, https://doi.org/10.3389/fendo.2021.680328.
[41] V. Karageorgiou, D. Kaplan, Porosity of 3D biomaterial scaffolds and osteogenesis, Biomaterials 26 (2005) 5474–5491, https://doi.org/10.1016/j.biomaterials.2005.02.002.
[42] D.M.R. Gibbs, C.R.M. Black, J.I. Dawson, R.O.C. Oreffo, A review of hydrogel use in fracture healing and bone regeneration, J. Tissue Eng. Regen. Med. 10 (2016) 187–198, https://doi.org/10.1002/term.1968.
[43] S.S. Lee, J.H. Kim, J. Jeong, S.H.L. Kim, R.H. Koh, I. Kim, S. Bae, H. Lee, N. S. Hwang, Sequential growth factor releasing double cryogel system for enhanced bone regeneration, Biomaterials 257 (2020), 120223, https://doi.org/10.1016/j.biomaterials.2020.120223.
[44] R. Subbiah, A. Cheng, M.A. Ruehle, M.H. Hettiaratchi, L.E. Bertassoni, R. E. Guldberg, Effects of controlled dual growth factor delivery on bone regeneration following composite bone-muscle injury, Acta Biomater. 114 (2020) 63–75, https://doi.org/10.1016/j.actbio.2020.07.026.
[45] L. Li, M. Yu, Y. Li, Q. Li, H. Yang, M. Zheng, Y. Han, D. Lu, S. Lu, L. Gui, Synergistic anti-inflammatory and osteogenic n-HA/resveratrol/chitosan composite microspheres for osteoporotic bone regeneration, Bioact. Mater. 6 (2021) 1255–1266, https://doi.org/10.1016/j.bioactmat.2020.10.018.
[46] I. Denry, O.-M. Goudouri, D.C. Fredericks, A. Akkouch, M.R. Acevedo, J. A. Holloway, Strontium-releasing fluorapatite glass-ceramic scaffolds: structural characterization and in vivo performance, Acta Biomater. 75 (2018) 463–471, https://doi.org/10.1016/j.actbio.2018.05.047.